IEEE Access
Multidisciplinary | Rapid Review | Open Access Journal

Received June 24, 2019, accepted August 13, 2019, date of publication August 20, 2019, date of current version September 5, 2019.

Digital Object Identifier 10.1109/ACCESS.2019.2936445

A Novel Method for Reconstructing Flatness Error Contour of Long Surface Based on a Laser Displacement Sensor

ZECHEN LU, ZHENJUN LI, (Member, IEEE), AND CHUNYU ZHAO
School of Mechanical and Automation, Northeastern University, Shenyang 110819, China

Corresponding author: Chunyu Zhao (chyzhao@mail.neu.edu.cn)

This work was supported by the National Natural Science Foundation of China under Grant 51775094.

ABSTRACT In order to solve the problem that the flatness error contour curve of the guideway mounting surface on machine tools can not be intuitive description, a novel method is proposed in this paper. The principle is to divide the measured surface with a certain length into several short surfaces with overlapping region, and the segmented surfaces are measured respectively, then the flatness error contours of the segmented surfaces can be obtained, finally, the segmented flatness error contours are spliced together to reconstruct the flatness error contour of the entire surface. On this basis, the detection instrument is designed, the detection principle is given, the benchmark plate is customized to identify the starting position and ending position of measurement, the reference surface and the measured surface are measured respectively in combination with the detection instrument and the benchmark plate. Then, an algorithm is developed to convert the distance difference between the reference surface and the measured surface into the flatness error contours of segmented surfaces. Next, using the geometric relationship between overlapping region of segmented flatness error contours, an algorithm is studied which can splice these segmented flatness error contours and reconstruct the flatness error contour of the entire surface. Meanwhile, mathematical models of the algorithms are established, and the measurement experiment is carried out. The results demonstrate that this method can reconstruct the flatness error contour of long surface accurately.

INDEX TERMS Flatness detection, machine tool, detection instrument, flatness error contour reconstruction, contour splicing.

I. INTRODUCTION

Accuracy of guideway mounting surfaces on machine tools is the foundation for ensuring the assembly error of the feed system [1]. It is also one of the crucial factors that determine the shape error and position error of workpiece. Nowdays, the detection of domestic machine tools still use traditional methods, such as dial gauges, level gauges, flat gauges, etc. But these methods have large randomness and are highly influenced by operator's proficiency and experience, it is impossible to describe the continuous distribution of assembly errors in the feed system, and it is difficult to quantify the influence of assembly errors on the dynamic characteristics of the feed system. In addition, during the detection process, the operators can only judge the quality by observing the variation range of the dial gauge, so that the local characteristic and the overall variation curve of the measured surface can not be understand, and it brings some difficulties to the dressing of the workpiece. Therefore, it is of great practical significance for manufacturing industry to depict the flatness error contour curve of the guideways mounting surfaces on machine tools.

At present, scholars at home and abroad have made great researches on straightness and flatness. You *et al.* [2] presented a method for measuring straightness error of beam bending compensation based on finite element thermal analysis. Zhou *et al.* [3] used the line-structured light vision method to realize the contour reconstruction of the rail. Hwang *et al.* [4] proposed a three-probe system, which can be utilized to acquire the parallelism and straightness of a pair of guideways simultaneously. Okuyama *et al.* [5] proposed a new two-point method for straightness profile measurement.

The associate editor coordinating the review of this article and approving it for publication was Tao Liu.

Su *et al.* [6] proposed a two-probe time domain method. Gao *et al* [7] describes a scanning multi-probe system for measuring straightness profiles of cylinder workpieces. Vladan Radlovački *et al.* [8] proposed a new method for evaluating minimum zone flatness error. Liu *et al.* [9] proposed a method for accurately measuring the flatness error of large and thin silicon wafers using a floating technique. Ehret *et al.* [10] established two new scanning deflection flatness reference measurement systems. Moreover, optical measurement can be made using an optical axis or laser beam determined by an optical accessory as a linear reference [11], [12]. The method of sensor combined with the flat crystal can realize the surface straightness error profile reconstruction of the guide rail [13]. Not only that, digital coordinate machines are also widely used in the flatness measurement. The number of sampling points is a key factor in determining the accuracy of flatness evaluation, excessive sampling points are the guarantee of detection accuracy [14]. For a large number of detection data, experts have proposed a variety of optimization algorithms for flatness evaluation, such as a support vector regression method [15], vectorial method [16] and a hybrid method based on reduced constraint region and convex-hull edge [17].

However, the above methods need to be carried out in a specific equipment and in a specific environment, the layout of the measurement system is very complex and needs enough space, and the measuring length of coordinate machine is limited, these methods are not suitable for measuring the long surface of machine tools with limited operating space. On the other hand, the commonly used detection devices, such as scanning probe or sensor, its detection position is a series points that cannot reflect the change of the surface shape in the width direction of the measured plane, therefore, the existing methods can not describe the flatness error contour curve of guideways mounting surface on machine tools. In order to solve this problem, a novel method was proposed in this paper. Meanwhile, a measuring instrument with a simple structure, convenient operation, small occupy space and suitable for manual operation is designed. This instrument combined with the splicing measurement method is an effective way to solve the problem that the flatness error profile curve of positioning surface on machine tools can not be described. Considering that the laser displacement sensor has the characteristics of simple structure, high resolution and real-time recording the data [18], it was selected as the detection component, Nevertheless, in order to reconstruct the flatness error contour of a long plane under the condition of the instrument designed in this paper, only the measurement method of piecewise stitching can be used. Due to the systematic error of the instrument, the benchmark plate needs to be added as the system error separation medium, and it is also used to identify the starting position of the measurement. Then, the segmented flatness error contour curve of the coincidence region can be obtained by the algorithms. It is known that the flatness error contours of overlapping areas are the same in theory. Using this principle, the flatness error contours of the whole surface can be joined together by an algorithm. In order to measure conveniently, the flatness of long surface is generally understood as the maximum straightness error of any section, which is called the flatness error contour.

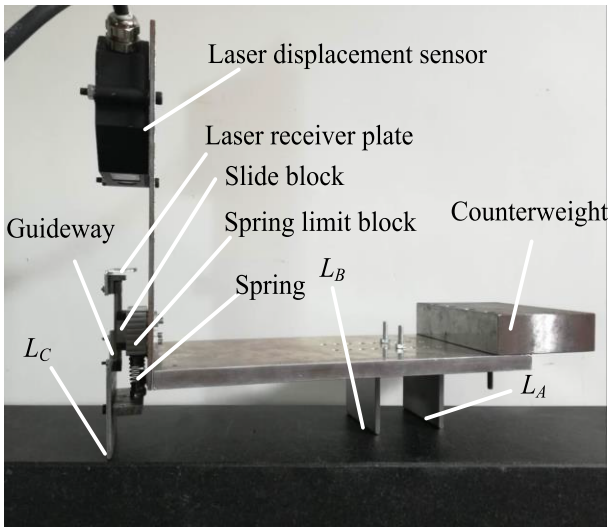

FIGURE 1. Flatness detection instrument.

The organization of this paper is as follows. Section II introduces the principle of the detection instrument and benchmark plate. Section III depicts the reconstruction process of flatness error contour. Section IV develops a series of algorithms. In Section V, this detection method is verified by experiments and the detection results are analyzed. Finally, the conclusion is given in Section VI.

II. PRINCIPLE

A. PRINCIPLE OF DETECTION INSTRUMENT

Fig.1 shows the flatness detection instrument. The detection instrument is balanced by a counterweight. L_A and L_B are fixed contact lines, and L_C is compressed on the measured surface through the spring. Contact lines L_A, L_B, and detection line L_C are grinded after processing, so that they have very high accuracy. The slider block is fixed on the instrument. L_C is integrated with the guideway and the laser receiving plate. The distance between L_A and L_B is 50mm, the distance between L_B and L_C is 180mm, the resolution of the laser displacement sensor is 0.3um, and the sampling frequency is 20kHZ.

In the detection process, the operator drives the detection instrument along the detection direction. L_C fluctuates with the flatness error contour of the measured surface, meanwhile, the guideway drives the laser receiver plate to fluctuate up and down, the sensor detects the undulation and records it through the computer. The detection result is a normal plane projection waveform along the onward direction of the detection instrument. The advantage of this mechanism is that it saves space and easy to operate, it can continuously obtain the stored data which changes with the flatness error profile

of the measured surface, instead of points on the same straight line along the measuring direction, which can not be achieved by the existing detection equipments.

B. PRINCIPLE OF BENCHMARK PLATE

Fig.2 shows the structure of the benchmark plate. The upper surface provides two grooves of a given depth for identifying the starting and ending positions of measurements, and the lower surface of the benchmark plate is flat(with extremely high machining accuracy). The length of the benchmark plate is 220mm and the distance between l_{O1} and l_{O2} is 200mm.

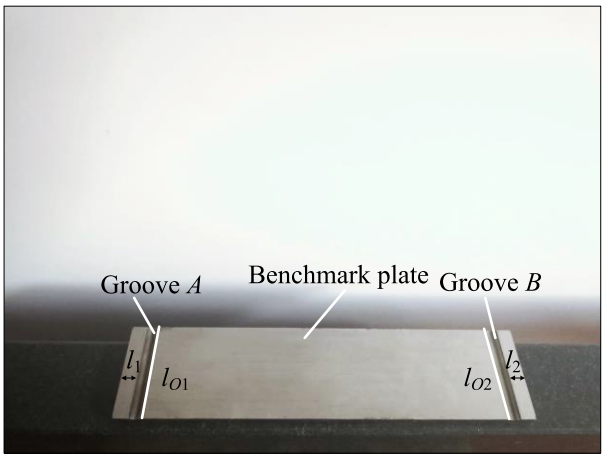

FIGURE 2. Benchmark plate.

Before measuring from left to right, L_A is in the l_1 area, and the detection instrument is manually pushed until the L_B sinks into the groove B. Before measuring from right to left, L_A is in the l_2 area, and the detection instrument is manually pushed until the L_B sinks into the groove A. The detection result is a waveform that changes with time, as shown in Fig.3.

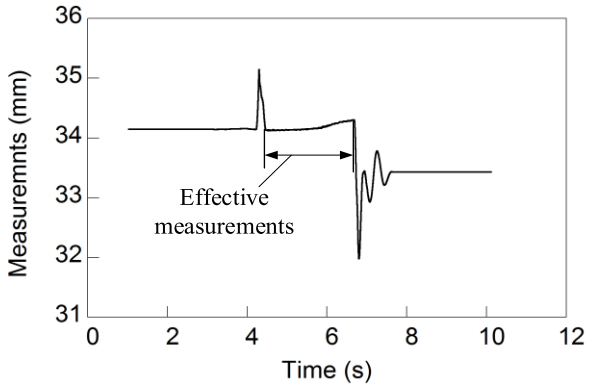

FIGURE 3. Measurements.

When the detection instrument is stationary, the detection result is a constant straight line. When the instrument passing through the groove, measurements generate a relatively obvious change. The contact lines L_A and L_B each pass through the groove once, generating one peak (L_A entering the groove) and one trough (L_B entering the groove). The measurements between the peaks and valleys are defined as an effective measurements. Before reconstructing flatness error contour, the measurements on both sides of l_{O1} and l_{O2} need to be separated to extract effective measurements.

III. RECONSTRUCTION PROCESS OF FLATNESS ERROR CONTOUR

A. EXTRACTING THE DETECTION CURVE OF THE REFERENCE SURFACE

Fig.4 shows the detection model of the reference surface. Due to there is a systematic error in the detection instrument, in order to separate it, assuming that the reference surface is an absolute horizontal surface, the systematic error can be separated by the distance difference between the measured surface and the reference surface. Therefore, in the process of reconstructing the flatness error contour of the measured surface, firstly, it is necessary to measure the reference surface. Based on the principle of the benchmark plate in section II.B, the benchmark plate is fixed on the reference surface and the reference surface is measured, the effective measurements can be extracted. Since the measurements are changing with time, then a time- space conversion algorithm is developed, and the time sequence measurements can be conversed to the spatial sequence measurements, that is, the measurements are changing with position. Owing to the flatness error contour is shape error, therefore, the trend curve of the spatial sequence measurements is extracted by the method of MATLAB neural network fitting, which is named as the detection curve of the reference surface.

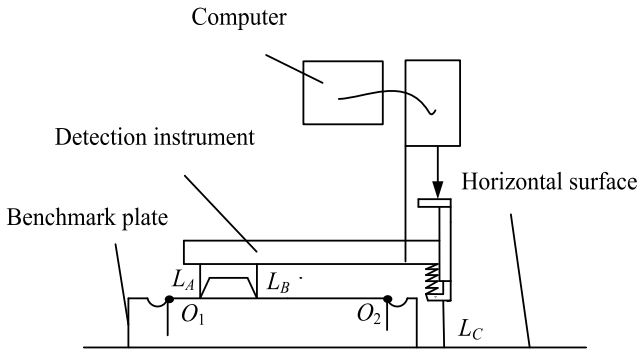

FIGURE 4. Detection model of the reference surface.

B. EXTRACTING THE SEGMENTED FLATNESS ERROR CONTOURS

Next, the benchmark plate is fixed on the measured surface. Fig.5 shows the detection model of measuring surface. Taking the length of the measured surface at 500mm and dividing it into five segments on average, the measurements of all the segmented surfaces are processed by the time- space conversion algorithm. When the benchmark plate O_1 and O_2 are respectively located at 0mm and 200mm, the detection instrument is pushed from left to right, the spatial sequence measurements corresponding to 230mm-380mm

can be obtained. When the benchmark plate O_1 and O_2 are located at 100mm and 300mm respectively, the detection instrument is pushed from left to right and from right to left respectively, and the spatial sequence measurements corresponding to 330mm-480mm and 70mm-0mm can be obtained. When the benchmark plate O_1 and O_2 are located at 200mm and 400mm respectively, the detection instrument is pushed from left to right and from right to left, the spatial sequence measurements corresponding to 430mm-500mm and170mm-20mm can be obtained. When the benchmark plate O_1 and O_2 are located at 300mm and 500mm respectively, the detection instrument is pushed from right to left, the spatial sequence measurements corresponding to 270mm-120mm can be obtained. Then the trend curves of all the space sequence measurements are extracted, which are called the detection curves of the measured surface. It can be seen from Fig.5 that there is a relative distance difference between the measured surface and the reference surface, therefore, the separating algorithm for reference surface detection curve is developed, and the flatness error contour of each segmented surface can be obtained. Owing to the flatness error contours of overlapping parts should be identical, the correctness of this detection method and the algorithms can be verified by the consistency of the flatness error contours of the overlapping regions.

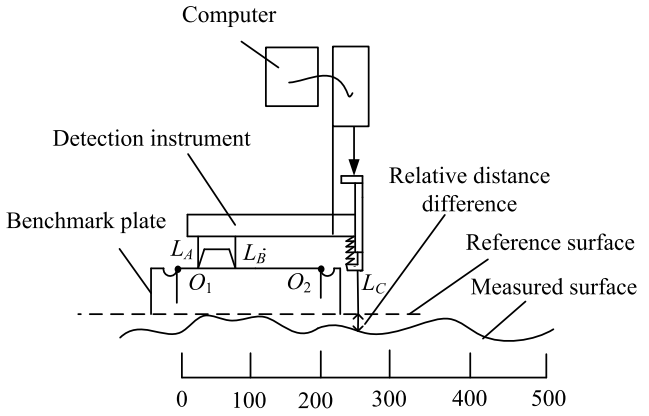

FIGURE 5. Detection model of the measured surface.

C. RECONSTRUCTING FLATNESS ERROR CONTOUR

This moment, the positions of the flatness error contours of segmented surfaces are shown in Fig.6. Then the splicing algorithm is developed. Using the geometric relationship between the contours of the overlapping region(the contours of the overlapping parts are identical), the adjacent two contours can be spliced together, finally, the flatness error contour of the entire measured surface can be reconstructed.

IV. NUMERICAL MODEL OF ALGORITHM

A. TIME-SPACE CONVERSION ALGORITHM

Since the detection results of the laser displacement sensor are changing over time, it is necessary to transform the time

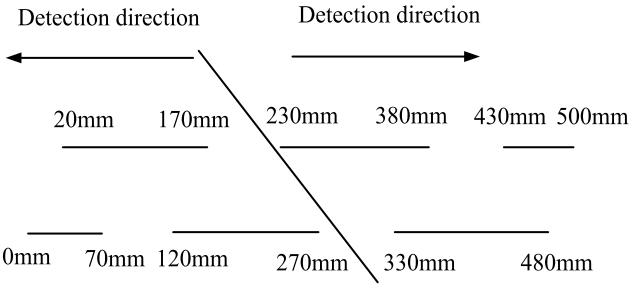

FIGURE 6. Positions of the segmented contours.

sequence measurements into the spatial sequence measurements. It is known that the moving speed of the detection instrument determines the number of measurements. Due to the frequency of the laser displacement sensor is 20kHz, it means that a certain measuring point may obtain dozens of data during the detection process. The essence of the time-space conversion algorithm is to filter the redundant data.

It is known that the detection time t can be defined as

$$t = \frac{N_L}{f} \tag{1}$$

where f represents the sampling frequency, N_L represents the number of measurements

Then the average velocity of the instrument can be defined as

$$v = \frac{L}{t} \tag{2}$$

where L represents the detection distance; t is derived from equation (1).

Let M represents the data set of the measurements. Then the variables a, e, w, s are created, the initial value of a is 1, $e = 1, 2, 3, \ldots, N_L$, $w = a, \cdots, N_L$, $s = M(a)$.

Then the equation (3) is defined as the objective function.

$$|M(w) - s| < d \tag{3}$$

where d is a given value; $M(w)$ represents the w-th data in the set M; The initial value of s is $M(1)$.

When $e = 1$, the equation (3) is executed to perform data search, when the searched data meets the condition of the objective function, $a = a + 1$, when the condition of the objective function is not meet, the data is stored, at this time, the redundant data is filtered out, and the equation can be expressed as follows

$$\left.\begin{aligned} F(e) &= a \\ K(e) &= M(a) \end{aligned}\right\} \tag{4}$$

where $F(e)$ represents the position of $K(e)$ in M; $K(e)$ represents stored data after filtering out redundant data.

Then perform new calculations on s, the equation can be expressed as

$$s = M(a) \tag{5}$$

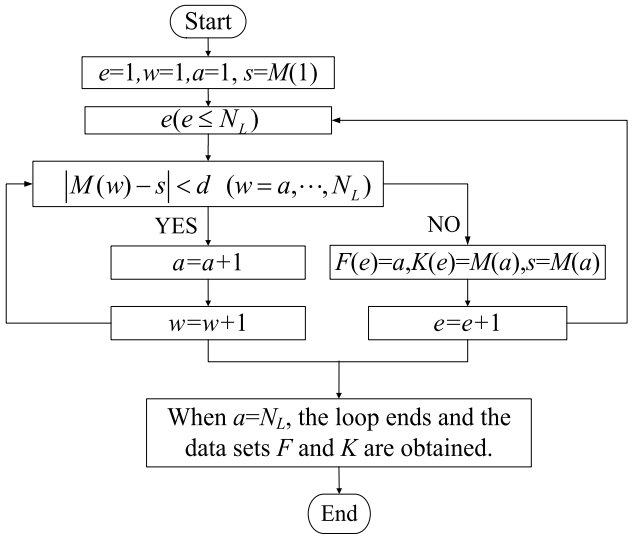

FIGURE 7. Flow chart of the algorithm.

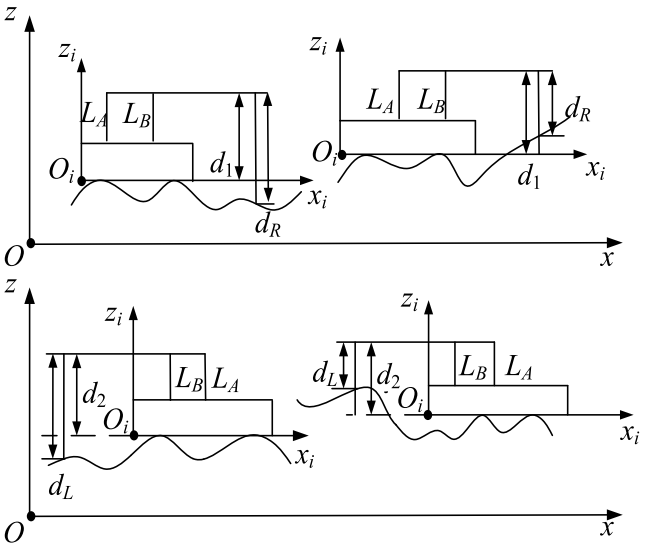

FIGURE 8. Separation algorithm model for detection curve of the reference surface.

After equation (5) is completed, $e = e + 1$, next, repeat execution equations (3)-(5), when $a = N_L$, the loop is completed. The flow chart of the algorithm is shown in Fig.7

At this time, the number of data in the sets F and K is N_c. It is known that the sampling interval of the measured surface is two sampling points with a certain value difference, so the detection time between the two sampling points can be expressed as

$$t_c(h) = \frac{F(h)t}{N_L} \tag{6}$$

where $F(h)$ represents the h-th data in set F, $h = 1, 2, 3, \ldots, N_c$; t is derived from equation (1);

The spatial sequence measurements can be obtained according to equation (7), so the time-space conversion of the data can be realized, and the equation (7) can be expressed as follows

$$\begin{aligned} vt_c(1) &\longrightarrow K(1) \\ vt_c(2) &\longrightarrow K(2) \\ vt_c(3) &\longrightarrow K(3) \\ &\cdots \\ vt_c(N_c) &\longrightarrow K(N_c) \end{aligned} \tag{7}$$

where v is derived from equation (2); $t_c(1, \cdots, N_c)$ is derived from equation (6); $K(1, \cdots, N_c)$ is derived from equation (4);

When measuring the reference surface, the spatial sequence measurements obtained by detection instrument moving from left to right is represented by C_1, the spatial sequence measurements obtained by detection instrument moving from right to left is represented by C_2, the trend curve of C_1 is defined as D_1, the trend curve of C_2 is defined as D_2.

When measuring the measured surface, the spatial sequence measurements of the j-th segmented surface obtained by detection instrument moving from left to right is represented by C_R^j, the spatial sequence measurements of the k-th segmented surface obtained by detection instrument moving from right to left is represented by C_L^k, the trend curve of C_R^j is defined as D_R^j, the trend curve of C_L^k is defined as D_L^k.

Then for ease of calculation, all trend curves are interpolated into the identical data structure, the equation can be expressed as

$$\begin{aligned} D_R^j &\xrightarrow{\text{Interpolation}(d_t)} d_R^j \\ D_L^k &\xrightarrow{\text{Interpolation}(d_t)} d_L^k \\ D_1 &\xrightarrow{\text{Interpolation}(d_t)} d_1 \\ D_2 &\xrightarrow{\text{Interpolation}(d_t)} d_2 \end{aligned} \tag{8}$$

where d_t represents sampling interval.

Under the condition that the sampling step is d_t, the number of sampling points N can be expressed as

$$N = \frac{L}{d_t} + 1 \tag{9}$$

where L represents the measuring distance of the detection instrument, and L is 150mm or 70mm.

B. SEPARATION ALGORITHM FOR DETECTION CURVE OF THE REFERENCE SURFACE

Fig.8 shows the model of separation algorithm for reference surface detection curve.

Take the measured surface in Fig 6 as an example, under the conditions of this model, we can know that j in equation (8) can take values 1, 2, 3, k in equation (8) can take values 1, 2, 3. Establish local coordinate systems $O_i x_i z_i$ at 0mm, 100mm,

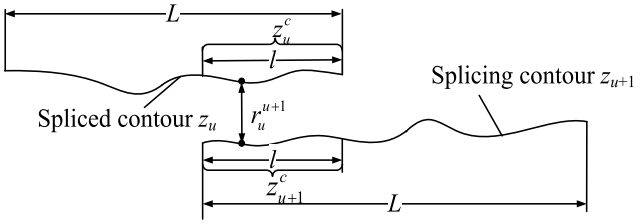

FIGURE 9. Splicing algorithm model.

200mm, 300mm of the measured surface, the variable i can take values 1,2,3,4, then establish global coordinate system Oxz at 0mm. x represents the direction of detection, z represents the deviation of the detection curve. The model contains all situations during the detection process.

When pushing the detection instrument from left to right to detect the measured surface, the j-th flatness error contour of the measured surface can be expressed as

$$z_R^j(n) = \pm \left| d_R^j(n) - d_1(n) \right| \tag{10}$$

where d_R^j and d_1 can be derived from equation 8, $d_R^j(n)$ represents the n-th data in d_R^j; $d_1(n)$ represents the n-th data in d_1; when $d_R^j(n) > d_1(n)$, uses $'-'$, when $d_R^j(n) < d_1(n)$, uses $'+'$, $n = 1, 2, 3, \ldots, N$;

The x coordinate corresponding to the contour $z_R^j(n)$ can be expressed as

$$x_R^j(n) = x_{O_i} + x_A(n) \tag{11}$$

where x_{O_i} represents the x-coordinate of O_1 in the global coordinate system, $x_A(n) = 0, d_t, 2d_t, 3d_t, \cdots L$; $n = 1, 2, 3, \ldots, N$.

Similarly, when pushing the detection instrument from right to left to detect the measured surface, the k-th flatness error contour of the measured surface can be expressed as

$$z_L^k(n) = \pm \left| d_L^k(n) - d_2(n) \right| \tag{12}$$

where d_L^k and d_2 can be derived from equation 8, $d_L^k(n)$ represents n-th data in d_L^k; $d_2(n)$ represents the n-th data in d_2; when $d_L^k(n) > d_2(n)$, uses $'-'$; when $d_L^k(n) < d_2(n)$, uses $'+'$; $n = 1, 2, 3, \ldots, N$;

The x-coordinate corresponding to the contour $z_L^k(n)$ can be expressed as

$$x_L^k(n) = x_{O_i} - 30 - x_A(n) \tag{13}$$

where x_{O_i} represents the x-coordinate of O_1 in the global coordinate system, $x_A(n) = 0, d_t, 2d_t, 3d_t, \ldots L$, $n = 1, 2, 3, \ldots, N$.

Finally, the flatness error contours of the segmented surfaces are represented by $z_1, z_2, z_3, z_4, z_5, z_6$, the corresponding detection positions are 0mm-70mm, 20mm-170mm, 120mm-270mm, 230mm-380mm, 330mm-480mm, 430mm-500mm.

C. SPLICING ALGORITHM

After obtaining the flatness error contours of the segmented surfaces, the overlapping regions of the two segments are subjected to polynomial fitting respectively. Ideally, the tangent slope of the curve at every point of the coincident region should be equal, however, the actual overlapping area contours can not be identical. Therefore, a splicing algorithm for finding the most suitable splicing point in the overlapping region is proposed.

Since the contour length l of the overlap region is known, the total number of sampling points of the overlap region can be expressed as

$$N_l = \frac{l}{d_t} + 1 \tag{14}$$

The splicing algorithm model is shown in Fig.9, the data set of overlapping area of the u-th spliced contour is set to z_u^c, the polynomial fitting equation is set to P_u, the data set of overlapping area of the $(u+1)$-th splicing contour is set to z_{u+1}^c, the polynomial fitting equation is set to P_{u+1}, then the tangent slope of each point in the overlapping area of the spliced contour z_u can be expressed as

$$S_u(n_l) = P_u(n_l)' \tag{15}$$

where $n_l = 1, 2, 3, \cdots N_l$; $u = 1, 2, 3, 4, 5$;

The tangent slope of each point in the overlapping area of the splicing contour z_{u+1} can be expressed as

$$S_{u+1}(n_l) = P_{u+1}(n_l)' \tag{16}$$

Then the equation (17) is defined as the objective function.

$$Q(n_l) = |S_{u+1}(n_l) - S_u(n_l)| \tag{17}$$

Extract the minimum value $Q(m)$ in the objective function, this point is the m-th data in n_l. It means that the overlap region contour has the smallest matching error at this position. This moment, the data in z_u is reselected to form a new spliced contour z_p, the equation can be expressed as

$$z_p = z_u\{1, 2, 3, \cdots, \frac{L}{d_t} - (\frac{l}{d_t} - m)\} \tag{18}$$

Then the data in z_{u+1} is reselected to form a new splicing contour z_{p+1}, the equation can be expressed as

$$z_{p+1} = z_{u+1}\{m, m+1, m+2, m+3, \cdots, \frac{L}{d_t} + 1\} \tag{19}$$

The splicing distance can be expressed as

$$r_u^{u+1} = z_u^c(m) - z_{u+1}^c(m) \tag{20}$$

The flatness error contour after the new splicing contour z_{p+1} transformation can be expressed as

$$z_p^{p+1} = z_{p+1} \pm \left| r_u^{u+1} \right| \tag{21}$$

when $r_u^{u+1} > 0$, uses $'+'$; when $r_u^{u+1} < 0$, uses $'-'$.

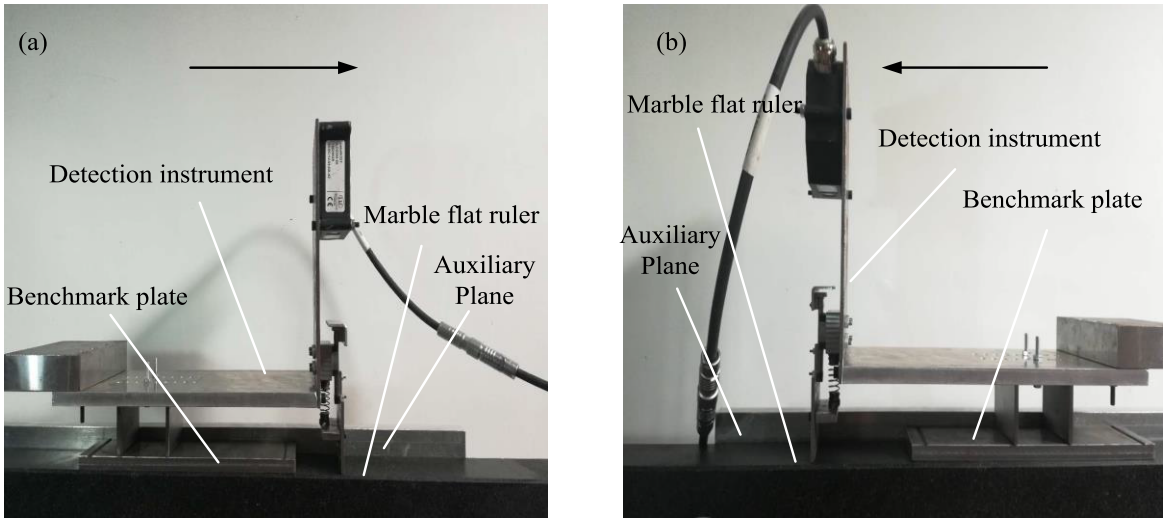

FIGURE 10. Detection system of the reference surface. (a) Detection instrument moves from left to right. (b) Detection instrument moves from right to left.

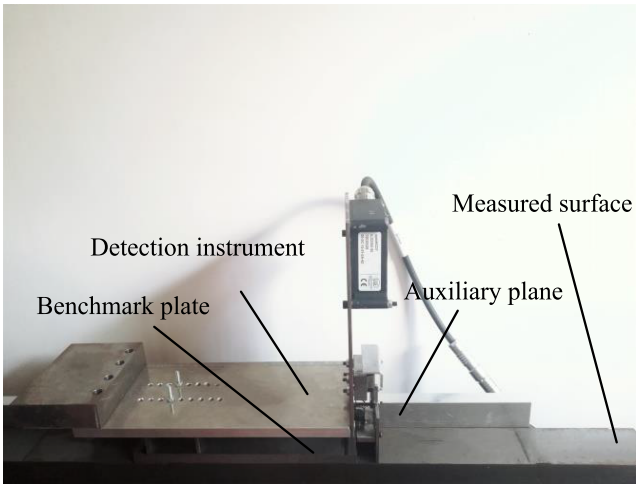

FIGURE 11. Detection system of the measured surface.

The adjacent two contours are joined together and the equation can be expressed as

$$z = \left\{ z_P, z_p^{p+1}(2, 3, \cdots, N) \right\} \tag{22}$$

Repeat the above process to splice the flatness error contour of each segment, and finally the whole flatness error contour of the measured surface can be reconstructed.

V. EXPERIMENTAL VERIFICATION

A. EXPERIMENTAL STEP

In order to verify the correctness of the detection method and algorithm, the measurement experiment was carried out. The surface of the marble flat ruler with a precision of 000 was selected as the reference surface.

Step 1, the benchmark plate was fixed on the surface of the marble flat ruler, according to the principle of benchmark plate in section II.B, the detection instrument was pushed three times from left to right and from right to left along the auxiliary surface respectively. The detection system of the reference surface is shown in Fig.10.

Step 2, the benchmark plate was fixed on the measured surface, the detection instrument moves along the positioning surface, and the measured surface with a length of 500mm was detected for three times according to the detection method of the measured surface in section III.B. The detection system of the measured surface is shown in Fig.11.During the measurement process, the measurement instrument moves along the auxiliary plane.

B. RESULTS AND ANALYSIS

According to the principle of benchmark plate in section II.B, effective time sequence measurements can be extracted from the detection data. By detecting the marble flat ruler, extracted effective time sequence measurements when the detection instrument driving from left to right are shown in Fig.12(a), extracted effective time sequence measurements when the detection instrument driving from right to left are shown in Fig.12(b). When detecting the measured surface, extracted effective time sequence measurements are shown in Fig.13. It can be seen from Fig.12 and Fig.13 that the measurements change with time and have a randomness.

Then the time-space conversion algorithm is used to process the time sequence measurements to obtain the spatial sequence measurements. Fig.14 shows the spatial sequence measurements of the reference surface, and Fig.15 shows the spatial sequence measurements of the measured surface. It can be seen from the Fig.14 and Fig.15 that the conversed measurements change with position, and due to the unstable motion of the detection instrument during the detection process, the waveforms of the three sets of spatial sequence

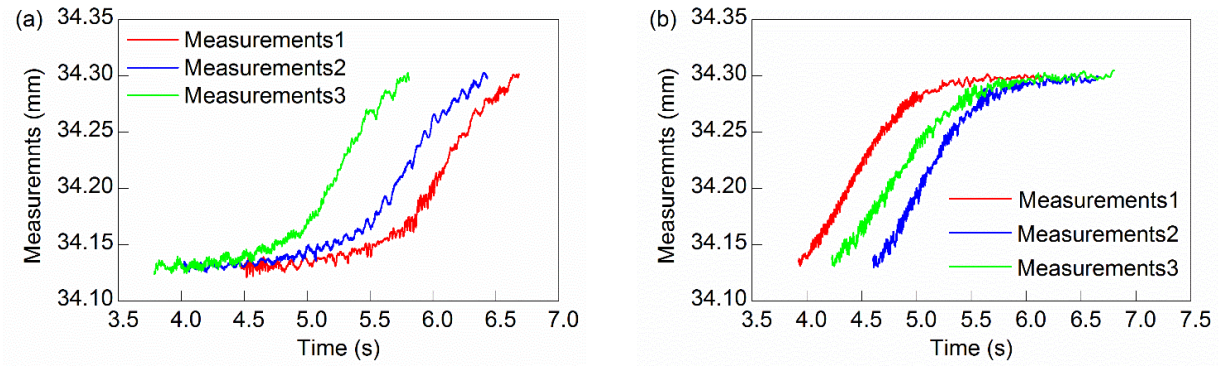

FIGURE 12. Time sequence measurements of reference surface. (a) Detection instrument moves from left to right. (b) Detection instrument moves from right to left.

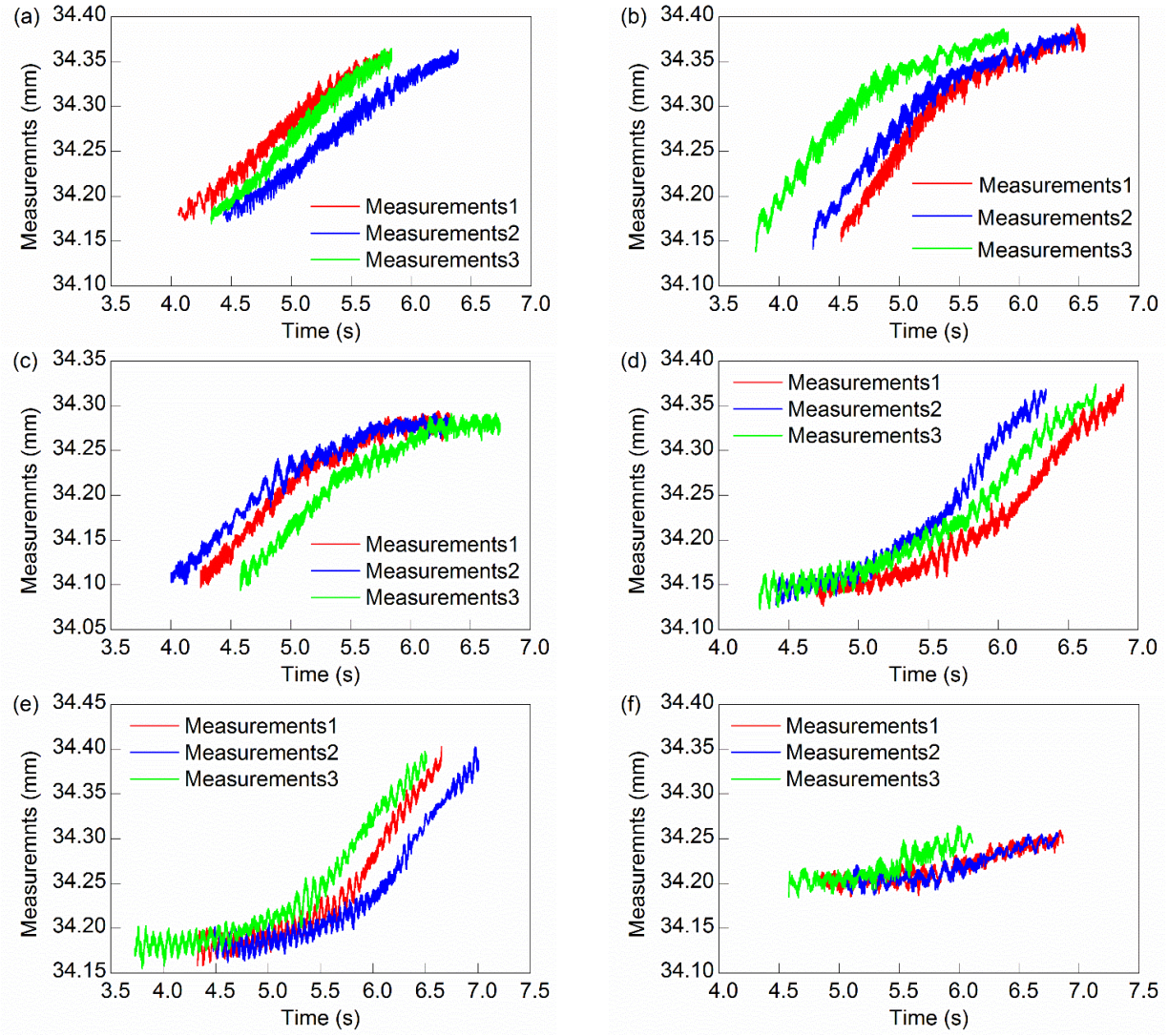

FIGURE 13. Time sequence measurements of the measured surface. (a) 70mm-0mm. (b) 120mm-20mm. (c) 270mm-120mm. (d)230mm-380mm. (e) 330mm-480mm. (f) 430mm-500mm.

measurements are different, but the overall shape is similar, which verifies the correctness of the time-space conversion algorithm.

Due to the flatness is shape error, therefore, the trend curves in Fig.14 and Fig.15 are extracted, which are called the detection curve. Fig.16 shows the detection curves of

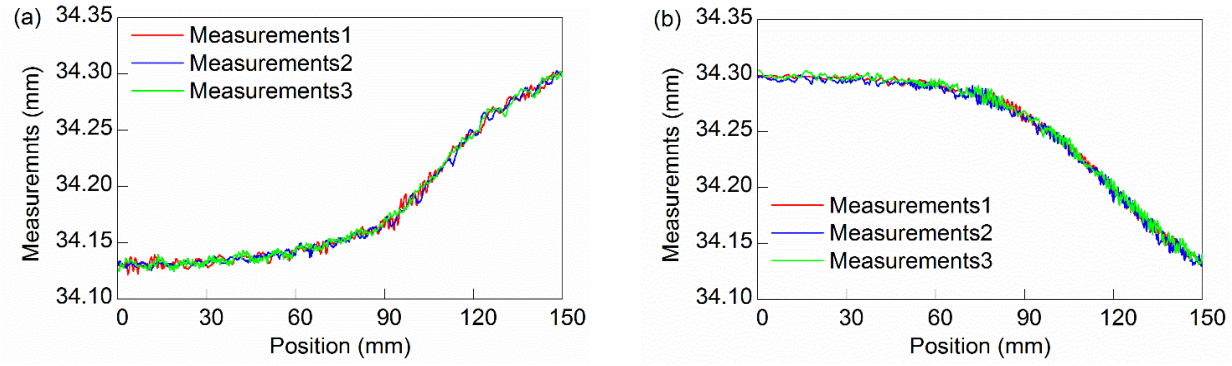

FIGURE 14. Spatial sequence measurements of the reference surface. (a) Detection instrument moves from left to right. (b) Detection instrument moves from right to left.

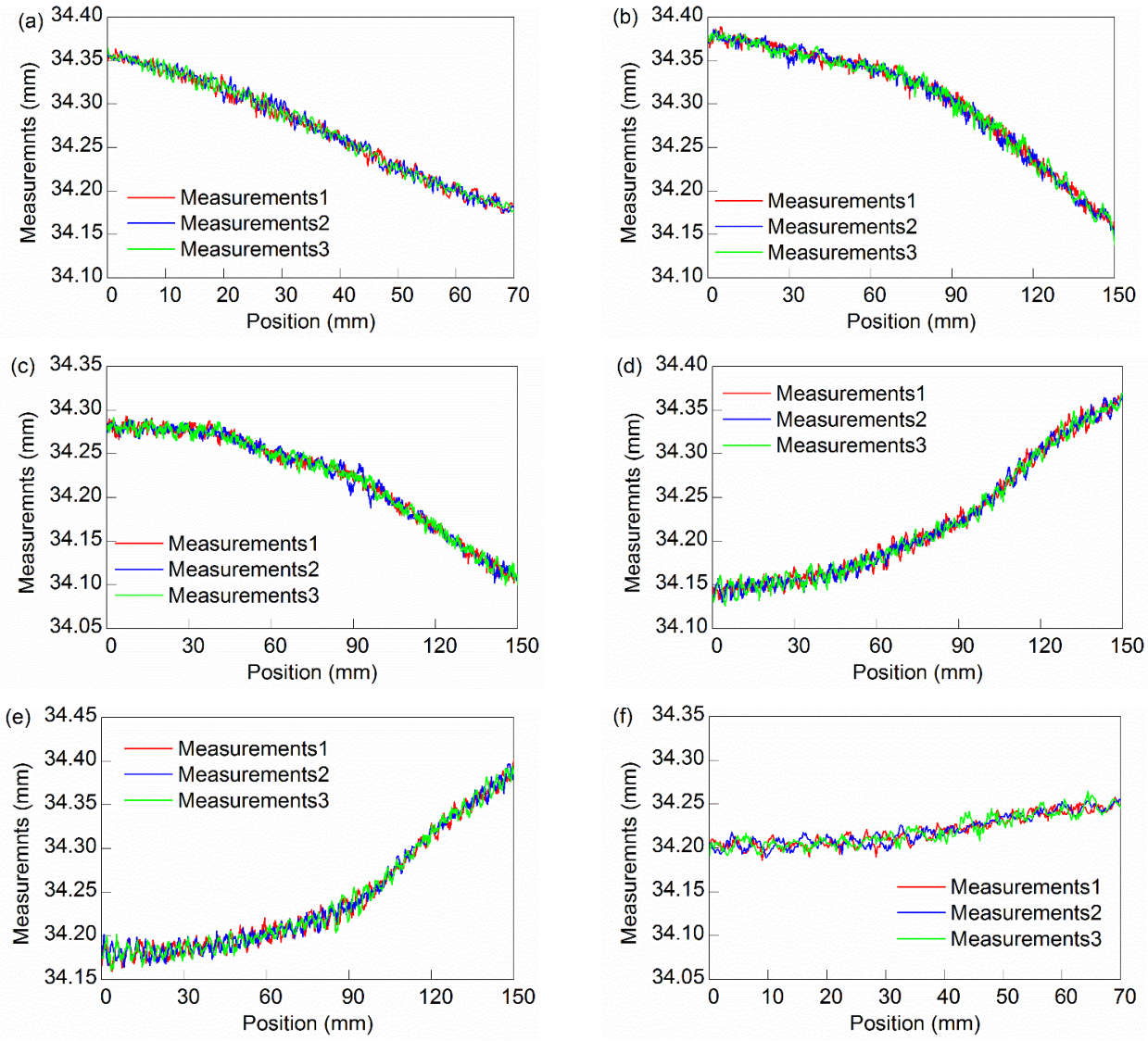

FIGURE 15. Spatial sequence measurements of the measured surface. (a) 0mm-70mm. (b) 20mm-170mm. (c) 120mm-270mm. (d)230mm-380mm. (e) 330mm-480mm. (f) 430mm-500mm.

the reference surface. Fig.17 shows the detection curves of measuring surface. It can be seen from Fig.16 and Fig.17, when the detection instrument repeatedly detects the identical surface, the detection lines L_A, L_B and L_C always pass the identical flatness error contour, so the detection curves at the same measuring path are close to coincidence.

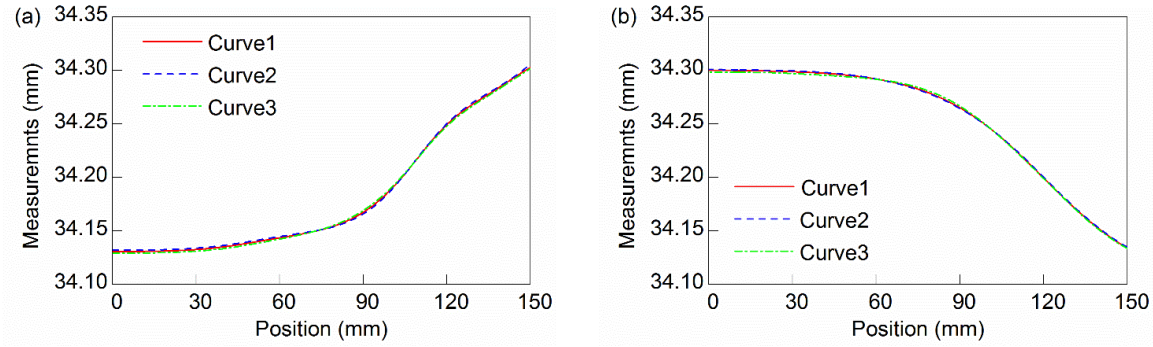

FIGURE 16. Detection curve of reference surface. (a) Detection instrument moves from left to right. (b) Detection instrument moves from right to left.

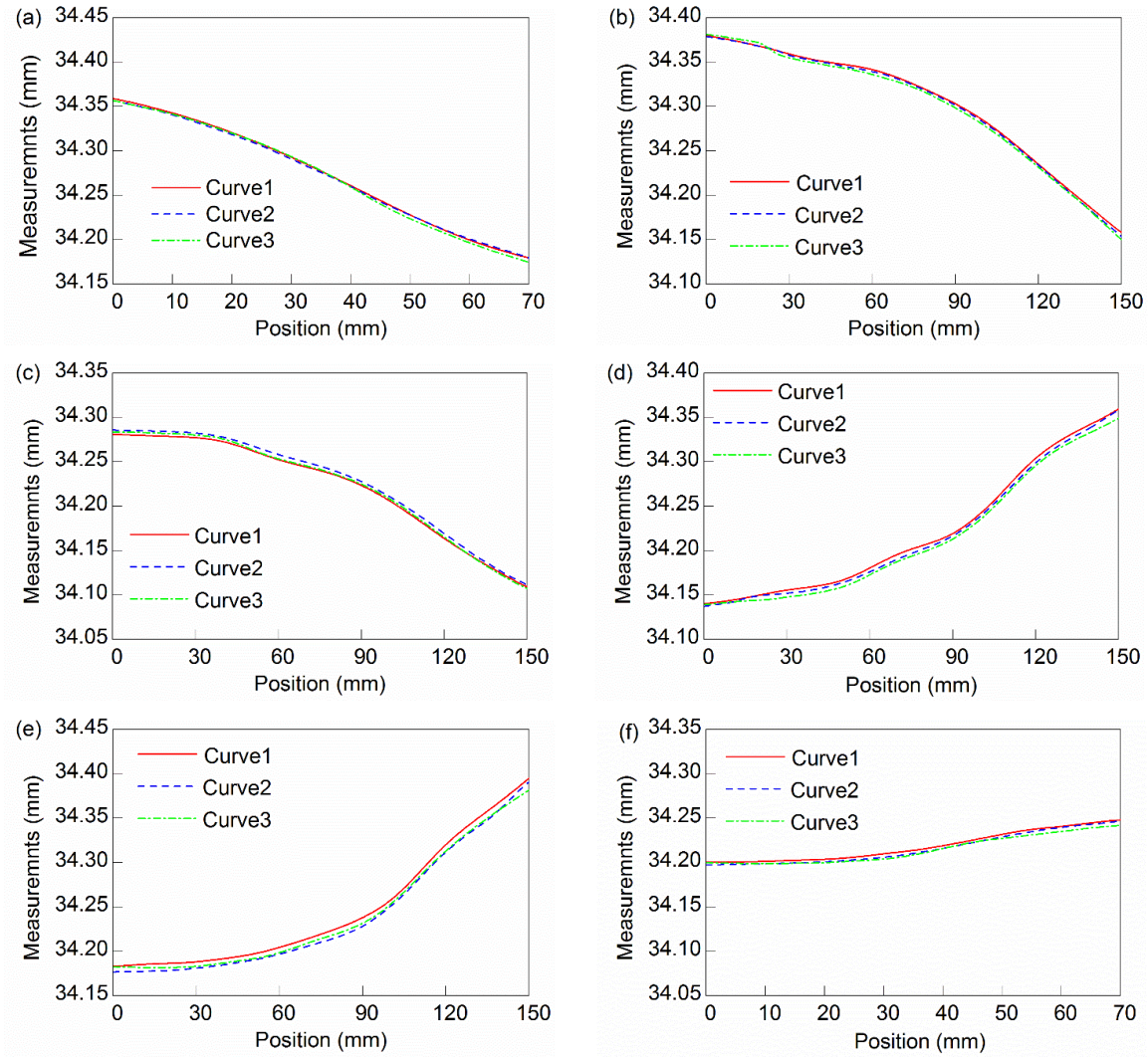

FIGURE 17. Detection curves of the measured surface. (a) 0mm-70mm. (b) 20mm-170mm. (c)120mm-270mm. (d)230mm-380mm. (e) 330mm-480mm. (f) 430mm-500mm.

Taking the average in Fig. 16(a) and Fig. 16(b) as the standard reference surface detection curve, then the standard detection curve and the curves in Fig.17 are processed using the separation algorithm of the reference surface detection curve. The obtained flatness error contours of the segmented surfaces are shown in Fig.18. It can be seen from Fig.18 that the segmented flatness error contours have overlapping portions, and the curve shape of each overlapping region is

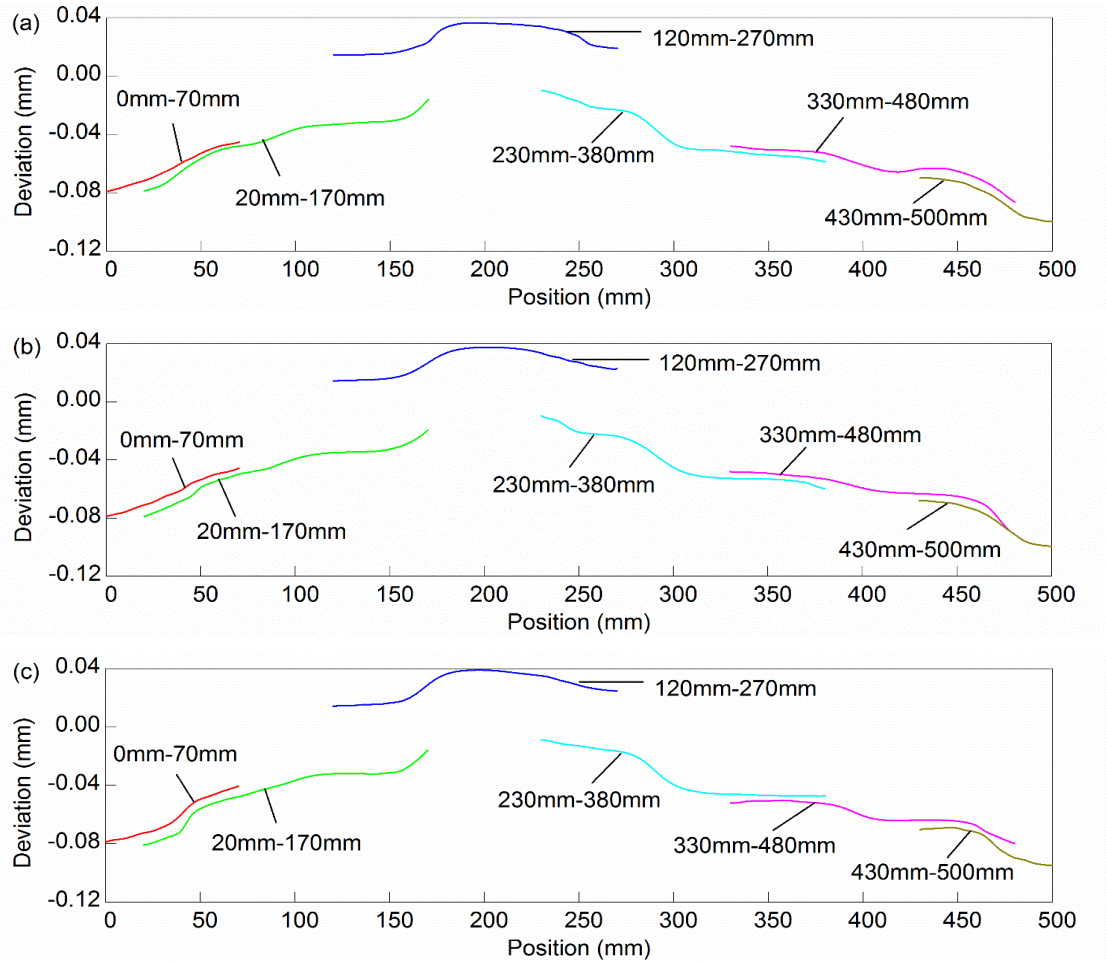

FIGURE 18. The segmented contours of the measured surface. (a) First group. (b) Second group. (c) Third group.

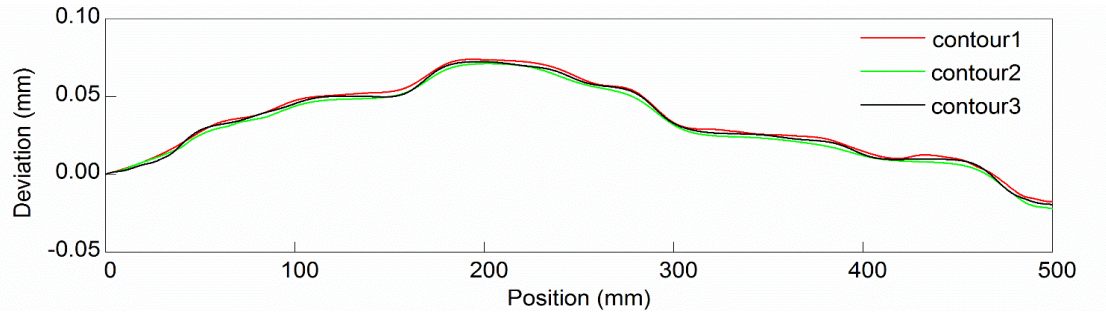

FIGURE 19. Reconstructed flatness error contour.

similar, which satisfies the verification method in section III.B. It means that we have correctly obtain the flatness error contours of the actual segmented surfaces, which verify the rationality of the detection method and the correctness of the separation algorithm.

Finally, the contours in Fig.18 are spliced using the splicing algorithm. The reconstructed flatness error contours of the measured surface are shown in Fig.19. It can be seen from Fig.19.The three reconstructed contours have a high similarity. Besides, the dimensional tolerance of the contour 1 is 91.53μm, the dimensional tolerance of the contour 2 is 92.38μm, and the dimensional tolerance of the contour 3 is 93.25μm. The maximum difference of the three reconstructed contours is 4.13μm, which is about 4.47% of the average dimensional tolerance. The result verifies the correctness of the splicing algorithm, and also shows that this method can

reconstruct the flatness error contour of the long surface accurately.

C. DISCUSSION

It can be seen from the measurements of the marble flat ruler, since the surface accuracy of the marble flat ruler is high, therefore the fluctuation of the measurements are little, the difference between the three sets of detection curves is tiny, so the average of detection curves can be used as a standard detection curve of reference surface. Similarly, improving the accuracy of the reference surface helps improve measurement accuracy. It can be seen from the measurements of the measured surface, the measurements of the measured surface fluctuate more obvious than that of the marble flat ruler. It is known that the shape of the extracted detection curve is determined by the measurements, since the detection pattern of this method is contact measurement, therefore improving the processing accuracy of the contact lines L_A, L_B, L_C and the benchmark plate surface can effectively reduce the fluctuation of the measurements, so that the extracted detection curve is closer to the real detection curve. Meanwhile, the higher accuracy of the lower surface of the reference plate, the actual contact relationship is closer to the detection model in section 3.2, the flatness error contours of segmented surfaces are closer to the true contours. Due to the result of the contour splicing is only related to the contour shape of the overlapping region, so the similarity of the overlapping region contours can be improved under the condition of improving the above requirements, so that the reconstructed flatness error contour can be more accurate.

VI. CONCLUSION

In this paper, a novel method for reconstructing the flatness error contour of long surface is proposed. Moreover, the time –space conversion algorithm, separation algorithm for detection curve of the reference surface, splicing algorithm for segmented contours were successfully developed. The experimental results demonstrate that this method can reconstruct the flatness error contour of long surface very well, and the design of the detection instrument is rational and the detection method is correct, which is operable in practical application. Compared with the traditional measurement method, this method can intuitively depict the flatness error contour curve. Compared with the existing research methods, the instrument is simple and convenient to operate, and takes up less space, which is more suitable for the measurement of machine tools. This research is of great significance for realizing on-site detection, real-time control and digital assembly required by modern industry.

REFERENCES

[1] J. Hong, J. Guo, Z. Liu, and X Wu, "Assembly accuracy prediction and adjustment process modeling of precision machine tool based on state space model," (in Chinese), *J. Mech. Eng.*, vol. 49, no. 6, pp. 114–121, Mar. 2013.

[2] F. You, B. Zhang, and Q. Feng, "A novel laser straightness measurement method with beam bend compensation," *Optik*, vol. 122, no. 17, pp. 1530–1534, Sep. 2011.

[3] P. Zhou, K. Xu, and D. Wang, "Rail profile measurement based on line-structured light vision," *IEEE Access*, vol. 6, pp. 16423–16431, 2018.

[4] J. Hwang, C.-H. Park, W. Gao, and S.-W. Kim, "A three-probe system for measuring the parallelism and straightness of a pair of rails for ultra-precision guideways," *Int. J. Mach. Tools Manuf.*, vol. 47, nos. 7–8, pp. 1053–1058, Jun. 2017.

[5] E. Okuyama, H. Akata, and H. Ishikawa, "Multi-probe method for straightness profile measurement based on least uncertainty propagation (2nd report)—Two-point method considering cross-axis translational motion, pitch motion and sensor's random error," *Precis. Eng.*, vol. 34, no. 4, pp. 683–691, Oct. 2010.

[6] H. Su, M. S. Hong, Z. J. Li, Y. L. Wei, and S. B. Xiong, "The error analysis and online measurement of linear slide motion error in machine tools," *Meas. Sci. Technol.*, vol. 13, no. 6, pp. 895–972, May 2002.

[7] W. Gao, J. Yokoyama, H. Kojima, and S. Kiyono, "Precision measurement of cylinder straightness using a scanning multi-probe system," *Precis. Eng.*, vol. 26, no. 3, pp. 279–288, Jul. 2002.

[8] V. Radlovački, M. Hadźistević, B. Štrbac, M. Delić, and B. Kamberović, "Evaluating minimum zone flatness error using new method—Bundle of plains through one point," *Precis. Eng.*, vol. 43, pp. 554–562, Jan. 2016.

[9] H. Liu, Z. Dong, H. Huang, R. Kang, and P. Zhou, "A new method for measuring the flatness of large and thin silicon substrates using a liquid immersion technique," *Meas. Sci. Technol.*, vol. 26, no. 11, Oct. 2015, Art. no. 115008.

[10] G. Ehret, M. Schulz, M. Stavridis, and C. Elster, "Deflectometric systems for absolute flatness measurements at PTB," *Meas. Sci. Technol.*, vol. 23, no. 9, Jul. 2012, Art. no. 094007.

[11] V. Vekteris, M. Jurevicius, and V. Striska, "Two-dimensional straightness measurement using optical meter," *Opt. Eng.*, vol. 47, no. 12, p. 760, Dec. 2008.

[12] C. Fang and C. Chen, "Straightness measurement of guide rail based on optical scanning method," (in chinese), *Opt. Instrum.*, vol. 37, no. 2, pp. 95–99, Feb. 2015.

[13] J. Lide, Z. Ziwen, and L. Shengyi, "Measurement method of straightness error of a long ultra-precise guideway with a short benchmark," (in chinese), *Chin. J. Mech. Eng.*, vol. 44, no. 9, pp. 141–147, Sep. 2008.

[14] W.-S. Kim and S. Raman, "On the selection of flatness measurement points in coordinate measuring machine inspection," *Int. J. Mach. Tools Manuf.*, vol. 40, no. 3, pp. 427–443, Feb. 2000.

[15] P. Balakrishna, S. Raman, T. B. Trafalis, and B. Santosa, "Support vector regression for determining the minimum zone sphericity," *Int. J. Adv. Manuf. Technol.*, vol. 35, nos. 9–10, pp. 916–923, Jan. 2008.

[16] R. Calvo, E. Gómez, and R. Domingo, "Vectorial method of minimum zone tolerance for flatness, straightness, and their uncertainty estimation," *Int. J. Precis. Eng. Manuf.*, vol. 15, no. 1, pp. 31–44, Jan. 2014.

[17] P. Li, X.-M. Ding, J.-B. Tan, and J.-W. Cui, "A hybrid method based on reduced constraint region and convex-hull edge for flatness error evaluation," *Precis. Eng.*, vol. 45, pp. 168–175, Jul. 2016.

[18] B. Sun and B. Li, "Laser displacement sensor in the application of aero-engine blade measurement," *IEEE Sensors J.*, vol. 16, no. 5, pp. 1377–1384, Mar. 2016.

ZECHEN LU was born in Tieling, Liaoning, China, in 1991. He received the B.Eng. degree in mechanical engineering from Dalian Polytechnic University, Dalian, in 2014, and the M.S. degree in mechanical engineering from Northeastern University, Shenyang, China, in 2016, where he is currently pursuing the Ph.D. degree in mechanical engineering.

His research interests include flatness detection, parallelism detection, on-site measurement of geometric errors, and digital description of geometric relations.

ZHENJUN LI (M'19) was born in Siping, Jilin, China, in 1992. He received the M.Eng. degree in mechanical engineering from Dalian Jiaotong University, Dalian, China, in 2017. He is currently pursuing the Ph.D. degree in mechanical engineering with Northeastern University, Shenyang, China. His research interests include thermo-mechanical coupling analysis of machine tools and mechanical system dynamics.

CHUNYU ZHAO was born in Heishan, Liaoning, China, in 1963. He received the bachelor's degree in engineering from the Department of Mechanical Engineering, Harbin Ship Engineering College, in 1986, and the Ph.D. degree from Northeast University, in 1997.

Since July 1996, he has been a Teacher, an Associate Professor, and a Professor with Northeastern University. He is currently a Professor, a Doctor, and a Doctoral Supervisor with the College of Mechanical Engineering and Automation Chemistry, Northeast University. His research interests include mechanical system dynamics, intelligent control of mechanical systems, grain drying and storage ventilation control, and industrial process monitoring and automation control.